ISSN 1070-3284, Russian Journal of Coordination Chemistry, 2017, Vol. 43, No. 5, pp. 297–303. © Pleiades Publishing, Ltd., 2017.
Original Russian Text © E.A. Katlenok, A.A. Zolotarev, A.Yu. Smirnov, S.N. Ivanov, R.I. Baichurin, S.V. Makarenko, K.P. Balashev, 2017, published in Koordinatsionnaya Khimiya, 2017, Vol. 43, No. 5, pp. 301–307.

Structures and Optical and Electrochemical Properties of the Pt(II) and Pd(II) Complexes with Cyclometallated 2-Phenylbenzothiazole and 1,4,7-Trithiocyclononane

E. A. Katlenok[a], A. A. Zolotarev[b], A. Yu. Smirnov[b], S. N. Ivanov[b], R. I. Baichurin[a], S. V. Makarenko[a], and K. P. Balashev[a, *]

[a] *Gertsen Russian State Pedagogical University, St. Petersburg, Russia*

[b] *St. Petersburg State University, St. Petersburg, Russia*

**e-mail: k_balashev@mail.ru*

Received July 14, 2016

Abstract—The distorted square pyramidal structures of the Pt(II) and Pd(II) complexes with cyclometallated 2-phenylbenzothiazole and flexible 1,4,7-trithiocyclononane are shown by X-ray diffraction analysis, IR spectroscopy, and ^{1}H, $^{13}C\{^{1}H\}$, and ^{195}Pt NMR spectroscopy. The axial interaction of the d_{Z2} orbital of Pt(II) and Pd(II) with the S atom of 1,4,7-trithiocyclononane results in the temperature quenching of the intraligand phosphorescence of the cyclometallated complexes in a solution and the one-electron ligand- and metal-centered reduction and oxidation of the complexes with the formation of the relatively stable Pd(III) complex (CIF file CCDC no. 1483011).

Keywords: Pd(II) and Pt(II) complexes with metallated 2-phenylbenzothiazole and 1,4,7-trithiocyclononane, X-ray diffraction analysis, IR spectroscopy, ^{1}H NMR, ^{13}C NMR, ^{195}Pt NMR, optical absorption and emission spectroscopy, reduction and oxidation voltammograms of complexes

DOI: 10.1134/S1070328417040029

INTRODUCTION

The specifics of the electronic structures of the square cyclometallated complexes $[Pt^{II}(C\hat{}N)(L\hat{}L)]^{Z}$ ($(C\hat{}N)^{-}$ is the metallated ligand, and $(L\hat{}L)^{n}$ is the chelated ligand) phosphorescing at room temperature provides wide possibilities of their use in various optoelectronic devices [1–3]. At the same time, it was shown [4, 5] that the weak axial interaction of coordinated 1,4,7-trithiocyclononane with Pt(II) and Pd(II) resulted in a significant change in the optical and electrochemical characteristics of the cyclometallated Pt(II) and Pd(II) complexes.

In this work, we present the results of the comparative study using X-ray diffraction analysis; IR spectroscopy; ^{1}H, $^{13}C\{^{1}H\}$, and ^{195}Pt NMR spectroscopy; electronic absorption, emission, and excitation spectroscopy; and voltammetry of complexes $[Pt(Pbt)([9]aneS_3)]PF_6$ (**I**) and $[Pd(Pbt)([9]aneS_3)]PF_6$ (**II**) ({M(Pbt)} is cyclometallated 2-phenylbenzothiazole, and $[9]aneS_3$ is 1,4,7-trithiocyclononane).

{M(Pbt)} =

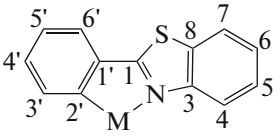

{M([9]aneS$_3$)} =

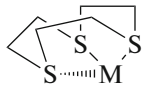

EXPERIMENTAL

Syntheses of complexes I and II were carried out using reagents (reagent grade), and the complexes were obtained in a yield of ~70%. Complex **I** was synthesized by reflux in an acetonitrile solution of $[Pt(Pbt)(\mu\text{-}Cl)]_2$ (1 equiv.) with $AgNO_3$ (2 equiv.) followed by the filtration of a precipitate of AgCl and the addition of $[9]aneS_3$ (1 equiv.) to the filtrate [6]. Complex **I** was precipitated by the addition of KPF_6 to the reaction mixture. A single crystal of complex **I** was obtained by the slow evaporation of a solution of the complex in dimethyl sulfoxide. Complex **II** was synthesized using a described procedure [4].

Hexafluorophosphate((2-phenyl-3-ido)benzothiazole)(1,4,7-trithiocyclononane)platinum(II) (**I**).

^{1}H NMR (CD_3CN), δ, ppm: {Pt(Pbt)}—8.08 d ($^3J_{HH}$ = 8.6 Hz, 2H^{4,7}), 7.76 m (H$^{6'}$), 7.68 dd ($^3J_{HH}$ = 8.4 Hz, 7.3, H^5), 7.62 m (H$^{4'}$), 7.55 dd ($^3J_{HH}$ = 8.0, 7.4 Hz, H^6), 7.31–7.27 m (2H$^{3',5'}$); {Pt([9]aneS$_3$)}—3.19–3.06 m (12H). ^{13}C{^{1}H} NMR ($(CD_3)_2SO$), δ, ppm: {Pt(Pbt)}—182.7 (C^1), 149.6 (C^3), 147.1 (C$^{2'}$), 139.6 (C$^{1'}$), 132.4 (C$^{3'}$), 132.6 (C$^{4'}$), 131.1 (C^8), 128.6 (C^5), 126.3 (C^6), 126.7 (C$^{6'}$), 125.3 (C$^{5'}$), 124.5 (C^7), 118.9 (C^4); {Pt([9]aneS$_3$)}—33.2. ^{195}Pt NMR (CD_3CN), δ, ppm: –3914.8.

Hexafluorophosphate((2-phenyl-3-ido)benzothiazole)(1,4,7-trithiocyclononane)palladium(II) (**II**). ^{1}H NMR (CD_3CN), δ, ppm: {Pd(Pbt)}—8.07 dd ($^3J_{HH}$ = 8.0 Hz, $^4J_{HH}$ = 0.7 Hz, H^4), 7.98 d ($^3J_{HH}$ = 8.4 Hz, H^7), 7.70 dd ($^3J_{HH}$ = 7.0 Hz, $^4J_{HH}$ = 2.0 Hz, H$^{6'}$), 7.64 ddd ($^3J_{HH}$ = 8.4, 7.3 Hz, $^5J_{HH}$ = 1.2 Hz, H^5), 7.53 td ($^3J_{HH}$ = 7.9 Hz, $^4J_{HH}$ = 0.9 Hz, H^6), 7.37 dd ($^3J_{HH}$ = 7.0 Hz, $^4J_{HH}$ = 1.9 Hz, H$^{3'}$), 7.27 td ($^3J_{HH}$ = 7.3 Hz, $^4J_{HH}$ = 1.3 Hz, H$^{4'}$), 7.24 td ($^3J_{HH}$ = 7.3 Hz, $^4J_{HH}$ = 1.8 Hz, H$^{5'}$); {Pd([9]aneS$_3$)}—3.18–3.03 m (12H). ^{13}C{^{1}H} NMR (CD_3CN), δ, ppm: {Pd(Pbt)} – 180.2 (C^1), 155.7 (C^3), 151.1 (C$^{2'}$), 141.3 (C$^{1'}$), 132.5 (C$^{3'}$), 132.6 (C$^{4'}$), 132.2 (C^8), 129.1 (C^5), 127.8 (C^6), 126.7 (C$^{6'}$), 127.2 (C$^{5'}$), 124.4 (C^7), 120.7 (C^4); {Pd([9]aneS$_3$)}—33.9.

The ^{1}H, ^{13}C{^{1}H}, dqf-COSY, ^{1}H–^{13}C HMQC, and ^{1}H–^{13}C HMBC spectra of the complexes in solutions of CD_3CN and $(CD_3)_2SO$ were recorded on a JNM-ECX400A spectrometer with working frequencies of 399.78 MHz (^{1}H) and 100.53 MHz (^{13}C) at the Center for Collective Use of the Gertsen Russian State Pedagogical University. Signals of residual protons of the non-deuterated solvent were used as an internal standard. The ^{195}Pt NMR spectra in a solution of CD_3CN (86.015 MHz) were obtained on a Bruker Avance III 400 spectrometer at the Resource Center "Magnetic Resonance Investigation Methods" of the St. Petersburg State University.

IR spectra in KBr pellets were measured on an IRPrestige-21 spectrometer. Absorption and emission spectra were recorded in acetonitrile on an SF-2000 spectrophotometer and a Flyuorat-02-Panorama spectrofluorimeter. Voltammograms were obtained on an ElinsPi-50-Pro setup in a cell with divided working (glassy carbon, GC), auxiliary (Pt), and reference (Ag) electrodes in a $C_6H_5CH_3$: CH_3CN (1 : 1) mixture in the presence of 0.1 M $[N(C_4H_9)_4]PF_6$. The peak potentials are presented at a rate of 100 mV/s with respect to the ferrocenium/ferrocene redox system.

X-ray diffraction analysis of complex I was carried out at 100 K on an Agilent Technologies Supernova single-crystal diffractometer (Resource Center "X-ray Diffraction Investigation Methods" of the St. Petersburg State University) with a CCD-type planar detector of reflected X rays (CuK_α, λ = 1.54184 Å). The crystallographic data and refinement parameters for structure **I** are presented in Table 1. The unit cell parameters were refined by least squares. The structure was solved by a direct method and refined using the SHELX program [7] with the OLEX2 complex [8]. An absorption correction was applied in the CrysAlisPro program package [9]. Hydrogen atoms were included into the refinement with fixed positional and temperature parameters. The structural information was deposited with the Cambridge Crystallographic Data Centre (CIF file CCDC no. 1483011; www.ccdc.cam.ac.uk/data_request/cif).

RESULTS AND DISCUSSION

Similarly to complex **II** [4], the X-ray diffraction analysis of complex **I** (Fig. 1) shows a distorted square pyramidal structure caused by the coordination of the third S atom in the axial position together with the coordination of the donor atoms of C,N-cyclometallated 2-phenylbenzothiazole and two atoms of S-endodentate 1,4,7-trithiocyclononane in the equatorial plane. The different natures of the donor atoms of C- and N-cyclometallated 2-phenylbenzothiazole and their *trans*-effect result in a difference of bond lengths of the metals with the donor atoms of the equatorial ligands: M–N and M–C by 0.06 Å and M–S(1) and M–S(2) by 0.12 and 0.09 Å for complexes **I** and **II**, respectively (Table 2).

The bond lengths of the metals with the S atom in the axial position are 3.00 and 2.91 Å, which is ~0.5 Å shorter than their sum of the van der Waals radii [10]. The intramolecular S–C and C–C bond lengths of coordinated 1,4,7-trithiocyclononane differ from those in the free ligand [11] less than by 0.01 Å. The platinum atom lies in the plane of the equatorial ligands, and the deviation of the axial S atom from the perpendicular position to the equatorial plane of the complex is 16.7°.

The position of the planes of the antisymmetric metallated ligands of adjacent complexes **I** and **II** with a dihedral angle between their planes of ~4° at a distance of ~3.5 Å is close to parallel, which determines the intermolecular π–π-stacking interaction of the phenyl and benzothiazole components of the ligands of the complexes (Fig. 1b).

The results of IR spectroscopy of the solid complexes shows the presence of both characteristic [12] frequencies of the mixed C=N/C=C and nonplanar bending C–H vibrations of metallated 2-phenylbenzothiazole and the C–S vibrations [13] of coordinated 1,4,7-trithiocyclononane (Table 3).

The ^{1}H and ^{13}C{^{1}H} NMR spectra of solutions of the complexes contain resonances of eight hydrogen atoms and 13 carbon atoms of the metallated ligand in the aromatic range. In spite of the chemical nonequivalence of the atoms of coordinated 1,4,7-trithiocyclo-

Table 1. Crystallographic and refinement parameters for the structure of $[Pt(Pbt)([9]aneS_3)]PF_6 \cdot (CH_3)_2SO$

Parameter	Value
Empirical formula	$C_{21}H_{26}F_6NOPPtS_5$
FW	808.79
Crystal system	Triclinic
Space group	$P\bar{1}$
Unit cell parameters:	
a, Å	8.3054(3)
b, Å	12.1038(3)
c, Å	14.7877(5)
α, deg	66.078(3)
β, deg	83.115(3)
γ, deg	74.444(3)
V, Å^3	1308.99(8)
Z	2
ρ_{calcd}, g/cm^3	2.052
μ, mm^{-1}	14.897
F(000)	788.0
Scan range over θ, deg	6.54–144.992
Index range	$-10 \le h \le 10, -14 \le k \le 10, -18 \le l \le 18$
Total number of reflections	15350
Independent reflections (R_{int})	5175 (0.0352)
GOOF	1.036
R factors ($F_0 \ge 4\sigma(F)$)	$R_1 = 0.0340$, $wR_2 = 0.0847$
R factors (all data)	$R_1 = 0.0357$, $wR_2 = 0.0863$
ρ_{min}/ρ_{max}, *e* Å^{-3}	4.13/–1.91

$R_1 = \Sigma||F_o| - |F_c||/\Sigma|F_o|$; $wR_2 = \{\Sigma[w(F_o^2 - F_c^2)^2]/\Sigma[w(F_o^2)^2]\}^{1/2}$; $w = 1/[\sigma^2(F_o^2) + (aP)^2 + bP]$, where $P = (F_o^2 + 2F_c^2)/3$; $s = \{\Sigma[w(F_o^2 - F_c^2)]/(n-p)\}^{1/2}$, *n* is the number of reflections, *p* is the number of refined parameters.

nonane in the complexes, the aliphatic range of the ^1H and ^{13}C NMR spectra of the complexes is characterized by a multiplet of 12 hydrogen atoms and one resonance of six carbon atoms of thiocrown ether. A decrease in the temperature of the solution to 183 K does not result in individual resonances of chemically nonequivalent 12 hydrogen atoms of coordinated 1,4,7-trithiocyclononane. This indicates a dynamic flexibility of coordinated 1,4,7-trithiocyclononane in the time scale of the detection of the NMR spectra of the complexes. A comparison of the coordinatively induced chemical shifts ($\delta_{comp}-\delta_{lig}$) of complexes **I** and **II** reflecting a change in the electron density of the atoms of the ligands upon coordination [14] shows (Table 4) an insignificant influence of the metal nature. The chemical shift of the platinum atom in the ^{195}Pt NMR spectrum of complex **I** ($\delta = -3914.8$ ppm) exhibits an upfield shift by 52 ppm compared to square [Pt(Pbt)(Dtc)] [15] (Dtc^- is the chelating diethyldithiocarbamate ion), which corresponds to some increase in the electron density of platinum in the complex with thiocrown ether.

The electronic absorption spectra of the complexes (Fig. 2) are characterized by two typical of the cyclometallated Pd(II) and Pt(II) complexes with metallated 2-phenylbenzothiazole [12, 15, 16] spin-allowed intense ($\varepsilon = (2-1) \times 10^4$ L mol^{-1} cm^{-1}) intraligand π–π* transitions and less intense ($\varepsilon = (8-2) \times 10^3$ L mol^{-1} cm^{-1}) *d*–π* metal-to-ligand charge transfer optical transitions localized on the metallocomplex fragment {M(Pbt)}. The position of the intraligand bands in the range <330 nm in the absorption spectra of the complexes is almost independent of the metal nature, whereas a decrease in the energy of the *d* orbitals of Pd(II) compared to Pt(II) results in the hypsochromic shift of the long-wavelength of the metal-to-ligand charge transfer absorption by ~1500 cm^{-1}. The metal-centered *d*–*d** absorption bands reflecting

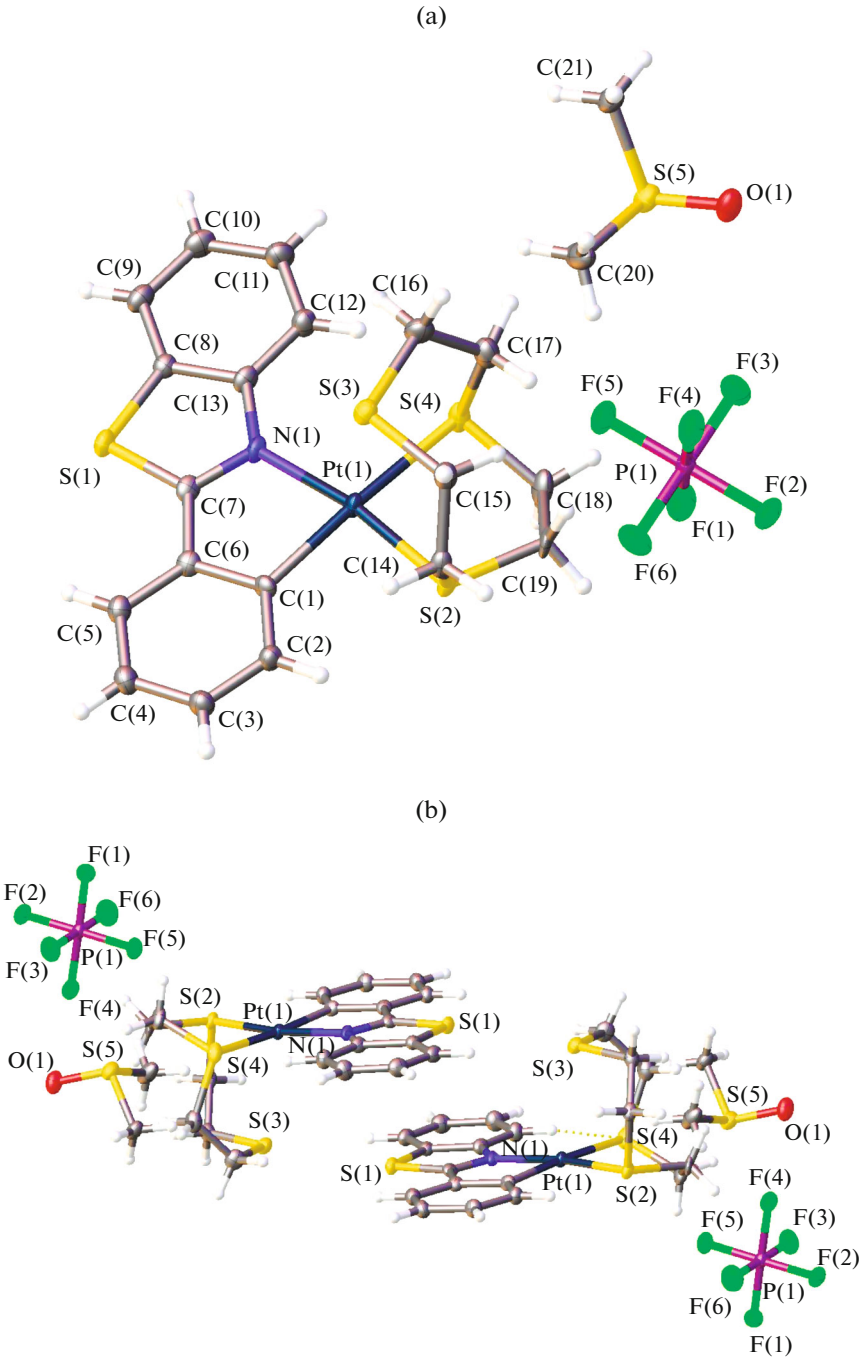

Fig. 1. (a) Molecular and (b) crystal structures of $[Pt(Pbt)([9]aneS_3)]PF_6 \cdot (CH_3)_2SO$. Thermal vibration ellipsoids are shown with 50% probability.

the optical transitions between the d_{Z2} and d_{X2-Y2} orbitals of the square pyramidal complexes [17] are hidden by more intense metal-to-ligand charge transfer optical transitions.

A specific feature of the Pt(II) complexes with cyclometallated 2-phenylbenzothiazole and 1,4,7-trithiocyclononane compared to the cyclometallated Pt(II) complexes is the complete quenching of phosphorescence upon the photoexcitation of liquid solutions of the complexes in the range of intraligand and metal-to-ligand charge transfer absorption bands. The luminescence of complexes **I** and **II** with the decay time 25 and 140 μs and vibration frequency 1410 ± 40 cm^{-1} is observed (Fig. 2) only in frozen (77 K) solutions. The vibration-structured character of the low-temperature luminescence of the complexes with the

Table 2. Bond lengths (*d*) and bond (ω) and torsion (τ) angles in $[Pt(Pbt)([9]aneS_3)]PF_6 \cdot (CH_3)_2SO$ and $[Pd(Pbt)([9]aneS_3)]PF_6 \cdot CH_3NO_2$ [4]

$[Pt(Pbt)([9]aneS_3)]PF_6 \cdot (CH_3)_2SO$			
Bond	*d*, Å	Bond	*d*, Å
Pt(1)–C(1)	2.040(5)	C(8)–S(1)	1.809(6)
Pt(1)–N(1)	2.095(4)	C(18)–S(1)	1.821(4)
Pt(1)–S(1)	3.001(1)	C(5)–S(2)	1.823(5) free 1.82
Pt(1)–S(2)	2.2522(9)	C(2)–S(2)	1.830(6)
Pt(1)–S(3)	2.366(1)	C(11)–S(3)	1.810(6)
C(2)–C(11)	1.509(7) free 1.51	C(19)–S(3)	1.837(5)
Bond angle	ω, deg	Bond angle	ω, deg
C(1)Pt(1)N(1)	80.7(2) (82.0(3))	S(1)Pt(1)S(2)	83.09(4)
S(2)Pt(1)S(3)	87.89(4)	S(1)Pt(1)S(3)	81.99(4)
Torsion angle	τ, deg		
S(2)Pt(1)S(3)S(1)	83.32(4)		
$[Pd(Pbt)([9]aneS_3)]PF_6 \cdot CH_3NO_2$			
Bond	*d*, Å	Bond	*d*, Å
Pd–C	2.033(5)	Pd–S_{ax}	2.909(2)
Pd–N	2.097(7)	*Trans* N Pd–S	2.285(2)
		Trans C Pd–S	2.380(2)

Table 3. Optical, IR, and electrochemical parameters for complexes $[Pt(Pbt)([9]aneS_3)]PF_6$ and $[Pd(Pbt)([9]aneS_3)]PF_6$

Complex	Electronic spectra			IR spectra			Potential	
	Absorption, λ_{max}, nm ($\varepsilon \times 10^3$ L mol^{-1} cm^{-1}; 293 K[a]	Emission λ_{max}, nm (τ, μs); 77 K[b]	Excitation λ_{max}, nm; 77 K[b]	ν, cm^{-1}			Ox $E_{1/2}$, V[c]	RedE_p, V[c]
				C=N/C=O	C–H	C–S		
I	248 (16.2), 265 sh (13), 310 sh (11), 324 (12.7), 355 (6.86), 379 (6.17), 425 sh (2.0)	517, 557, 604, 670 sh (25)	315 sh, 332, 345 sh, 383, 400 sh	1476	750	683, 668	0.26	1.87
II	254 (19.8), 265 sh (15), 318 (11.2), 355 sh (7.9), 400 sh (1.5)	509, 548, 596 (140)	312, 325 sh, 350 sh, 365, 388	1481	748	679, 668	0.60, 0.79	1.66

[a] CH_3CN, [b] C_4H_8O, [c] $C_6H_5CH_3 : CH_3CN$.

frequency close to the frequency of C=N/C=O vibrations of the benzothiazole component of the metallated ligand and a relatively long time of the luminescence decay indicates the spin-forbidden predominantly intraligand π–π* optical transition of the metallocomplex component {M(Bt)}. The bathochromic shift of the phosphorescence spectrum of the Pt(II) complex compared to that of Pd(II) by 300 cm^{-1} is due to an increase in the degree of admixing of the metal-to-ligand charge transfer to the intraligand excited state responsible for the phosphorescence of the complexes.

The temperature phosphorescence quenching of cyclometallated complexes **I** and **II** was assigned to the

Table 4. Coordinatively induced chemical shifts ($\delta_{comp}-\delta_{lig}$, ppm) of the atoms of the ligands in complexes $[Pt(Pbt)([9]aneS_3)]PF_6$ and $[Pd(Pbt)([9]aneS_3)]PF_6$

Complex	No.	1	3	4	1'	2'	3'	$[9]aneS_3$
I	^1H			−0.08			−0.3	0.06
	^{13}C*	15.2	−4.2	−4.2	6.5	19.7	2.9	−0.6
II	^1H			−0.09			−0.21	0.05
	^{13}C	12.7	1.9	−2.4	8.2	23.7	3.0	0.0

* $(CD_3)_2SO$.

temperature-activated occupation of a higher energy *d*–*d** excited state undergoing the fast chemical reaction [18, 19]. The axial interaction of the S atom of 1,4,7-trithiocyclononane with the d_{Z2} orbital of the metals favors a decrease in the energy of the *d*–*d** state, which determines a high efficiency of the temperature phosphorescence quenching of solutions of complexes **I** and **II**.

The reduction voltammograms of complexes **I** and **II** are characterized by the irreversible one-electron waves (Fig. 3) assigned to the ligand-centered electron transfer processes to the π* orbitals of {M(Pbt)} of the cyclometallated ligand followed by the chemical reaction:

$$[M(Pbt)([9]aneS_3)]^+ + e^- = [M(Pbt^-)([9]aneS_3)] \rightarrow \text{chemical reaction}. \quad (1)$$

Unlike the irreversible ligand-centered reduction waves, the oxidation voltammograms of the complexes are characterized by quasi-reversible waves (Table 4) assigned to the metal-centered electron transfer processes. Two one-electron waves corresponding to the consecutive oxidation of palladium and a relative stability of the $[Pd^{III}(Pbt)([9]aneS_3]^{2+}$ complex are observed for the Pd(II) complex (Fig. 3):

$$[Pd^{II}(Pbt)([9]aneS_3)]^+ - e^- = [Pd^{III}(Pbt)([9]aneS_3)]^{2+}, \quad (2)$$

$$[Pd^{III}(Pbt)([9]aneS_3)]^{2+} - e^- = [Pd^{IV}(Pbt)([9]aneS_3)]^{3+}. \quad (3)$$

The oxidation voltammogram of $[Pt(Pbt)([9]aneS_3]^+$ is characterized by one quasi-reversible one-electron wave (Fig. 3) with the formation, probably, of the Pt(III) complex undergoing the further chemical reaction:

$$[Pt^{II}(Pbt)([9]aneS_3)]^+ - e^- = [Pt^{III}(Pbt)([9]aneS_3)]^{2+} \rightarrow \text{chemical reaction}. \quad (4)$$

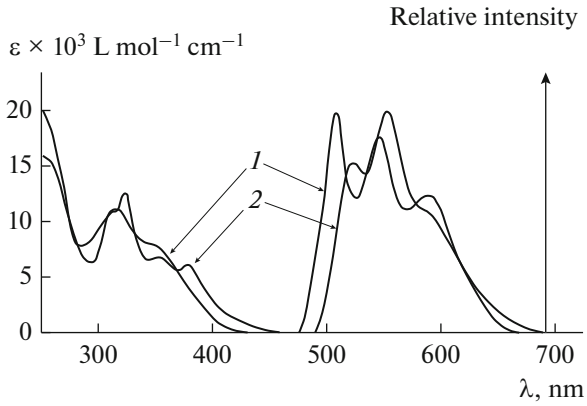

Fig. 2. Absorption and emission spectra of complexes (*1*) $[Pd(Pbt)([9]aneS_3)]PF_6$ and (*2*) $[Pt(Pbt)([9]aneS_3)]PF_6$.

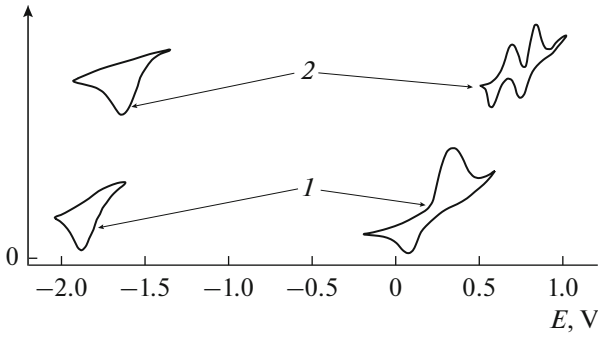

Fig. 3. Oxidation and reduction voltammograms of complexes (*1*) $[Pt(Pbt)([9]aneS_3)]PF_6$ and (*2*) $[Pd(Pbt)([9]aneS_3)]PF_6$.

A decrease in the difference of the oxidation and reduction potentials of the Pt(II) complexes compared to that of Pd(II) by 0.13 V shows a decrease in the energy gap between the highest occupied and lowest unoccupied molecular orbitals, which is consistent with the bathochromic shift in the absorption spectrum of the long-wavelength metal-to-ligand charge transfer optical transition of the Pt(II) complexes compared to that of Pd(II) by ~1500 cm^{-1}.

A similar one-electron oxidation of the Pd(II) and Pt(II) complexes with the formation of the relatively stable and unstable Pd(III) and Pt(III) complexes, respectively, was observed [5] for the oxidation of the cyclometallated complexes $[Pd(Bzq)([9]aneS_3)]^+$ and $[Pt(Bzq)([9]aneS_3)]^+$ (Bzq^- is cyclometallated benzo[h]quinoline).

The results of this work show that the axial interaction of the d_{Z2} orbital of Pt(II) and Pd(II) with the S atom of 1,4,7-trithiocyclononane leads to both the temperature quenching of the intraligand phosphorescence of the square pyramidal cyclometallated complexes in a solution and one-electron metal-centered oxidation with the formation of the relatively stable Pd(III) complex.

REFERENCES

1. Chi, Y. and Chou, P.-T., *Chem. Soc. Rev.*, 2010, vol. 39, no. 2, p. 638.
2. Fan, C. and Yang, C., *Chem. Soc. Rev.*, 2014, vol. 43, no. 17, p. 6439.
3. Williams, J.A.G., Develay, S., Rochester, D.L., et al., *Coord. Chem. Rev.*, 2008, vol. 252, nos. 23–24, p. 2596.
4. Jansen, D.A., Bruening, M.A., Sutton, C.A., et al., *J. Organomet. Chem.*, 2015, vol. 777, p. 31.
5. Jansen, D.A., Van Derveer, D.G., Mehne, L.F., et al., *Dalton Trans.*, 2008, no. 14, p. 1872.
6. Lamansky, S., Djurovich, P., Murphy, D., et al., *Inorg. Chem.*, 2001, vol. 40, no. 7, p. 1704.
7. Sheldrick, G.M., *Acta Crystallogr., Sect. A: Found. Crystallogr.*, 2008, vol. 64, no. 1, p. 112.
8. Dolomanov, O.V., Bourhis, L.J., Gildea, R.J., et al., *J. Appl. Crystallogr.*, 2009, vol. 42, no. 2, p. 339.
9. *CrysAlisPro. Agilent Technologies. Version 1.171.36.20 (release 27-06-2012)*.
10. Bondi, A., *J. Phys. Chem.*, 1964, vol. 68, no. 3, p. 441.
11. Glass, R.S., Wilson, G.S., and Setzer, W.N., *J. Am. Chem. Soc.*, 1980, vol. 102, no. 15, p. 5068.
12. Katlenok, E.A. and Balashev, K.P., *Opt. Spektrosk.*, 2013, vol. 114, no. 4, p. 114.
13. Fleming, G.D., Vallette, M.M.C., Clavijo, E., et al., *Spectrochimica Acta, Part A*, 1999, vol. 55, no. 9, p. 1827.
14. Orellana, J., Ibarra, C.A., and Santoro, J., *Inorg. Chem.*, 1988, vol. 27, no. 6, p. 1025.
15. Katlenok, E.A., Zolotarev, A.A., Ivanov A.Yu., et al., *Russ. J. Coord. Chem.*, 2016, vol. 42, no. 3, p. 178.
16. Katlenok, E.A. and Zolotarev, A.A., *Russ. J. Coord. Chem.*, 2015, vol. 41, no 1, p. 37.
17. Lever, A., *Inorganic Electronic Spectroscopy*, New York: Elesvier, 1984.
18. Sajioto, K., Djurovich, P.I., Tamayo, A.B., et al., *J. Am. Chem. Soc.*, 2009, vol. 131, no. 28, p. 9813.
19. Barigelletti, F., Sandrini, D., Maestri, M., et al., *Inorg. Chem.*, 1988, vol. 27, no. 20, p. 3644.

Translated by E. Yablonskaya